energies

MDPI

Article

An Experimental Comparison of the Performances of a Small Water-to-Water Heat Pump Working with R1234ze(E) and Its Mixture R515B †

Luca Molinaroli *, Andrea Lucchini and Luigi Pietro Maria Colombo

Dipartimento di Energia, Politecnico di Milano, Via Raffaele Lambruschini 4/A, 20156 Milano, Italy; andrea.lucchini@polimi.it (A.L.); luigi.colombo@polimi.it (L.P.M.C.)

* Correspondence: luca.molinaroli@polimi.it

† This paper is an extended version of our paper published in Colombo, L.P.M.; Frigerio, D.; Lucchini, A.; Molinaroli, L. Experimental assessment of the use of R515B as R1234ze(E) alternative in a small water-to-water heat pump. In the Proceedings of the 26th International Congress of Refrigeration, Paris, France, 21–25 August 2023.

Abstract: The study presents the results of an experimental investigation aimed at evaluating the performance of a water-to-water heat pump utilising R1234ze(E) and R515B in a drop-in application. Several operating conditions are tested, varying the mass flow rates and temperatures of the secondary fluids that pass through the heat exchangers while maintaining the compressor shaft rotational frequency and the vapour superheating at the evaporator outlet constant. Overall, when compared to R1234ze(E), the utilisation of R515B results in capacity and COP variations within −6.81% to +2.46% and −2.41% to +6.29%, respectively. Regarding the performance of the compressor, R515B exhibits comparable volumetric and overall efficiency, while a slightly lower refrigerant temperature at the compressor discharge is found, with differences ranging from −3.1 °C to −0.5 °C. Overall, R515B appears to be more suitable than R1234ze(E) for applications in the high-temperature range.

Keywords: compressor; COP; heat pump; heating capacity; R1234ze(E); R515B

Citation: Molinaroli, L.; Lucchini, A.; Colombo, L.P.M. An Experimental Comparison of the Performances of a Small Water-to-Water Heat Pump Working with R1234ze(E) and Its Mixture R515B. *Energies* **2024**, *17*, 5812. https://doi.org/10.3390/en17235812

Academic Editor: Artur Blaszczuk

Received: 24 September 2024
Revised: 19 November 2024
Accepted: 19 November 2024
Published: 21 November 2024

1. Introduction

Over the past decade, the air conditioning and refrigeration industry has initiated a transition away from traditional refrigerants to comply with regulations aimed at reducing greenhouse gas emissions. Specifically, the EU Regulation 517/2014 [1] and the Kigali Amendment to the Montreal Protocol [2] have introduced a gradual phase-out of high Global Warming Potential (GWP) refrigerants in favour of low-GWP alternatives. Consequently, environmentally friendly refrigerants are continuously being developed and proposed as substitutes for traditional Hydrofluorocarbons (HFCs) [3–5]. Among these, HydroFluoroOlefins (HFOs) have emerged as the most promising category of low-GWP refrigerants for vapour compression systems. HFOs are typically classified as A2L substances, indicating mild flammability. To shift their classification to A1, meaning non-flammable, HFOs are often blended with non-flammable HFCs [6].

One such blend, R515B, has been introduced as an alternative to pure HFOs like R1234ze(E). R515B is a mixture of R1234ze(E) (91.1% by weight) and R227ea (8.9% by weight), though it has received limited attention from the scientific community so far. At the system level, Mota-Babiloni et al. [7] experimentally compared the performance of R134a, R1234ze(E) and R515B in a water-to-water heat pump under identical evaporating and condensing conditions. Their findings suggest that compared to R1234ze(E), R515B offers slightly lower heating capacity while maintaining a comparable COP.

Similar results were found through a numerical study of the same refrigerants in a water-to-water heat pump designed for moderately high-temperature applications, in

which it is found that R515B provides slightly lower heating capacity and COP than R1234ze(E) [8].

At the component level, the refrigerant temperature at the compressor discharge and the compressor volumetric efficiency are analysed in [7], while the heat transfer performance was studied in [9–11]. From a compressor standpoint, the discharge temperature with R515B was found to be lower than with R1234ze(E), though both refrigerants exhibited similar volumetric efficiency [7]. In terms of heat transfer, R1234ze(E) and R515B displayed comparable convective heat transfer coefficients, with R1234ze(E) performing slightly better during condensation and R515B showing a slight advantage during evaporation [9–11].

The goal of this paper is to expand our previous study [12] about the analysis of the use of R515B in vapour compression systems discussing the results of experimental tests of a small-capacity, water-to-water heat pump. In the analysis, the inlet or outlet temperatures of the secondary fluids are set rather than the evaporating or condensing ones since according to [13], "a comparative analysis based on the same evaporation and condensation temperatures may not apply in some circumstances, since the refrigerant replacement will give rise to different temperatures for fixed conditions of the cooling medium in the condenser and the medium to be cooled". The final goal of the present paper is to contribute to the assessment of R515B as a viable, alternative refrigerant to R1234ze(E). This is achieved through a comprehensive experimental campaign carried out in a broad range of operating conditions, allowing us to understand which refrigerant among the two considered performs better and in what operating conditions. The present study aims at integrating the scientific literature about these refrigerants, allowing vapour compression system designers and manufacturers to make a rational choice among them.

2. Experimental Setup and Experimental Procedure

2.1. Experimental Setup

The experimental setup used in the present work was the same used in our previous studies, and therefore, only a short description is provided in the present paper, whereas more details are available in [14,15].

The layout of the experimental facility is shown in Figure 1.

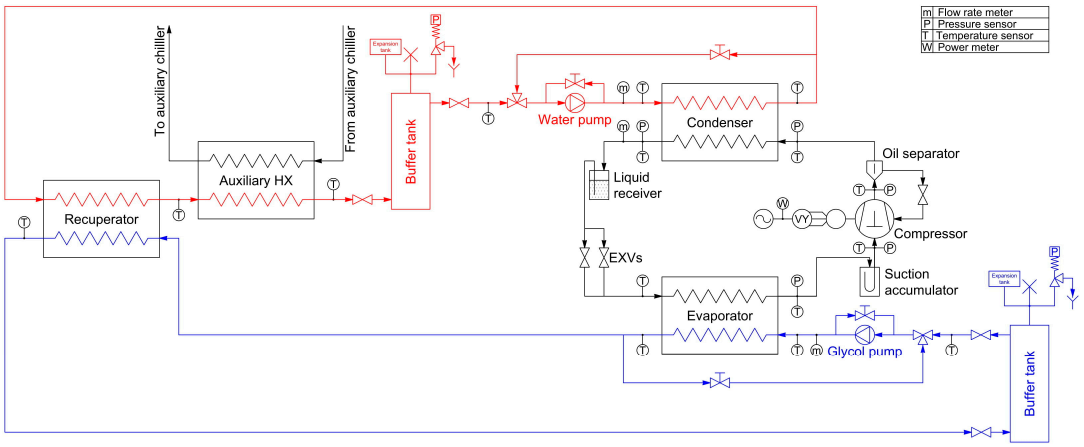

Figure 1. The layout of the experimental setup.

As per [15], the setup "consists of a refrigerant loop (heat pump, black line), a water loop (hot heat sink, red line) and a water + ethylene glycol loop (cold heat source loop, blue line) in which a mixture of water and ethylene glycol at concentration equal to 25.4%v with a freezing temperature equal to −12.6 °C is used.

The main components of the refrigerant loop are a variable speed, semi-hermetic reciprocating compressor, a brazed plate condenser, a brazed plate evaporator and two electronic expansion valves. The two expansion valves are different in size and are installed to enlarge the range of the capacities that can be tested. Only the most appropriate valve is

used during each test. In the refrigerant loop the controlled parameters are the rotational frequency of the compressor shaft and the vapour superheating at evaporator outlet.

The main components of the hot and cold secondary fluid loops are a variable speed pump, a buffer tank, a two-way and a three-way valve. In these loops the controlled parameters are the pump speed and the secondary fluid temperatures.

All the pipes and the components are insulated with an elastomeric material whose thermal conductivity is 0.037 W/(m·K).

The characteristics of the main components of the experimental facility are collected in Table 1, whereas the position of the measuring instrumentation and its main characteristic are reported in Figure 1 and Table 2 respectively.

Table 1. The main characteristics of the components of the experimental setup.

Component	Parameter	Value
Compressor	Swept volume @ 50 Hz Shaft rotational frequency Oil type Oil charge	13.15 m^3/h 30 Hz–87 Hz POE ISO 32 1.1 dm^3
Condenser	Dimensions Number of plates	289 mm × 119 mm × 93.6 mm 40
Evaporator	Dimensions Number of plates	376 mm × 119 mm × 71.2 mm 30
Expansion valves	Capacity range	175 W–1750 W 1690 W–16900 W
Pumps (both cold heat source and hot heat sink loops)	Nominal flow rate Nominal head Shaft rotational frequency	28.7 m^3/h 160 kPa 16 Hz–58 Hz

Table 2. Main characteristics of the measuring instrumentation (RTD = resistance Temperature Detector).

Parameter	Instrument	Range
Refrigerant mass flow rate	Coriolis mass flow meter (Endress Hauser, Cernusco sul Naviglio, Italy)	0 kg/h–300 kg/h
Refrigerant pressure (low side)	Pressure transducer (Huba Control, Würenlos, Switzerland)	0 kPa–700 kPa
Refrigerant pressure (high side)	Pressure transducer (Huba Control, Würenlos, Switzerland)	0 kPa–4000 kPa
Refrigerant temperature	RTD Pt 100 (Tersid, Sesto San Giovanni, Italy)	243.15 K–373.15 K
Compressor power	Power meter (Cewe, Nyköping, Sweden)	0 W–4000 W
Water mass flow rate	Vortex flow meter (Huba Control, Würenlos, Switzerland)	0.21 m^3/h–3 m^3/h
Water temperature	RTD Pt 100 (Tersid, Sesto San Giovanni, Italy)	263.15 K–353.15 K

2.2. Refrigerant Tested and Testing Conditions

The refrigerant tested in the present study was R515B, a mixture of R1234ze(E) (91.1%w) and R227ea (8.9%w), which is considered a drop-in substitute for R1234ze(E). The main properties of these refrigerants were retrieved from Refprop 10.0 [16] and are reported in Table 3.

The performance of the heat pump working with R515B was assessed considering 25 experimental points that spanned a broad range of working conditions. These testing conditions were the same used to characterise the operation of the heat pump with R1234ze(E) in our previous work [14]. Each test was carried out setting the compressor shaft rotational frequency to 50 Hz, setting the superheating at evaporator outlet to 5 K and

changing the temperatures of the secondary fluids at the evaporator and the condenser outlets as reported in Table 4. The mass flow rates of the secondary fluids were identified in 5 reference conditions (Tests 03, 08, 13, 18 and 23 in Table 4), setting a temperature drop (evaporator) or increase (condenser) change equal to 5 K. Once these flow rates were identified, 20 additional tests were carried out varying the temperatures of the secondary fluids at the heat exchanger outlets as per the combination reported in Table 4. It is worth mentioning that in these conditions, the inlet temperatures of the secondary fluids were not set but were identified depending on the operating conditions and the flow rates.

Table 3. Main properties of R1234ze(E) and R515B.

Parameter	R1234ze(E)	R515B
Composition	Pure	R1234ze(E) 91.1%w R227ea 8.9%w
Critical pressure	3634.9 kPa	3583.9 kPa
Critical temperature	382.51 K	382.03 K
Molar mass	114.04 g/mol	117.48 g/mol
$c_{P,0}$	95.13 J/(mol·K)	97.18 J/(mol·K)
Normal Boiling Point (Dew)	254.18 K	254.37 K
Glide (p = 101,325 kPa)	0 K	0.021 K
ODP (Ozone Depletion Potential)	0	0
GWP (Global Warming Potential) (IPCC 6th revision)	1.37	321
ASHRAE classification	A1	A1

Table 4. Testing conditions.

Test	Compressor	Evaporator			Condenser		
	f_{SHAFT}	$\dot{m}_G$	$T_{G,IN}$	$T_{G,OUT}$	$\dot{m}_W$	$T_{W,IN}$	$T_{W,OUT}$
1	50 Hz	As Test 03	*	268.15 K	As Test 03	*	308.15 K
2	50 Hz	As Test 03	*	273.15 K	As Test 03	*	308.15 K
3	50 Hz	Identified	283.15 K	278.15 K	Identified	303.15 K	308.15 K
4	50 Hz	As Test 03	*	283.15 K	As Test 03	*	308.15 K
5	50 Hz	As Test 03	*	288.15 K	As Test 03	*	308.15 K
6	50 Hz	As Test 08	*	268.15 K	As Test 08	*	318.15 K
7	50 Hz	As Test 08	*	273.15 K	As Test 08	*	318.15 K
8	50 Hz	Identified	283.15 K	278.15 K	Identified	313.15 K	318.15 K
9	50 Hz	As Test 08	*	283.15 K	As Test 08	*	318.15 K
10	50 Hz	As Test 08	*	288.15 K	As Test 08	*	318.15 K
11	50 Hz	As Test 13	*	268.15 K	As Test 13	*	328.15 K
12	50 Hz	As Test 13	*	273.15 K	As Test 13	*	328.15 K
13	50 Hz	Identified	283.15 K	278.15 K	Identified	323.15 K	328.15 K
14	50 Hz	As Test 13	*	283.15 K	As Test 13	*	328.15 K
15	50 Hz	As Test 13	*	288.15 K	As Test 13	*	328.15 K
16	50 Hz	As Test 18	*	268.15 K	As Test 18	*	338.15 K
17	50 Hz	As Test 18	*	273.15 K	As Test 18	*	338.15 K
18	50 Hz	Identified	283.15 K	278.15 K	Identified	333.15 K	338.15 K
19	50 Hz	As Test 18	*	283.15 K	As Test 18	*	338.15 K
20	50 Hz	As Test 18	*	288.15 K	As Test 18	*	338.15 K
21	50 Hz	As Test 23	*	268.15 K	As Test 23	*	348.15 K
22	50 Hz	As Test 23	*	273.15 K	As Test 23	*	348.15 K
23	50 Hz	Identified	283.15 K	278.15 K	Identified	343.15 K	348.15 K
24	50 Hz	As Test 23	*	283.15 K	As Test 23	*	348.15 K
25	50 Hz	As Test 23	*	288.15 K	As Test 23	*	348.15 K

* Temperature not set a priori but found depending on the operating conditions and on the identified flow rate.

2.3. Experimental Procedure

The experimental procedure used to carry out the experimental campaign was the following (adapted from our previous works [14,15]):

1. At the beginning of each test, the pumps of the cold water + ethylene glycol loop and of the hot water loop are switched on. The rotational frequency of each pump shaft is set to the value required to guarantee the mass flow rates needed by the test (see experimental conditions in Table 4). This value is continuously monitored during the test and is adjusted to keep the mass flow rate constant.
2. The compressor is switched on and its shaft rotational frequency is set to the value required by the test. At the same time, the electronic expansion valve begins to modulate its cross-section area in order to guarantee a superheating at evaporator outlet equal to 5 K.
3. The temperatures of the cold water + ethylene glycol and of the hot water that respectively flow through the evaporator and the condenser begin changing. In both the secondary fluid loops, a PID (Proportional Integral Derivative) controller acts on the 3-way valve with the aim of setting the secondary fluid temperature at heat exchanger outlet to the value required by the test. During the test, the PID controllers continuously adjust the 3-way valve position to keep the outlet temperatures to the set-point.
4. Once the set-point temperatures are reached, the data acquisition starts with a sampling frequency equal to 1 Hz. For each measured pressure and temperature, the moving average over the last 900 samples is computed. For each of them, the entire 900 samples batch is checked to lay within ±2.5 kPa (for the pressures) and ±0.2 K (for the temperatures) with respect to the just calculated moving average. When this constraint is simultaneously satisfied by all the measured pressures and temperatures simultaneously, the test is considered in steady-state condition.
5. Once steady-state operation is achieved, the data acquisition starts and further 900 samples are recorded for data analysis. An additional check of the accuracy of the test is performed at its end calculating the refrigerant-side and the secondary fluid-side heat transfer rates at the evaporator and at the condenser. The test is considered valid if the two values agree within ±4% with respect to their average value, otherwise it is repeated.

2.4. Data Reduction and Uncertainty Calculation

The analysis of the performance of the heat pump was carried out considering the following parameters: condenser heat transfer rate, heat pump coefficient of performance, refrigerant temperature at the compressor discharge, compressor volumetric efficiency and pinch points at the evaporator and at the condenser. These parameters were computed using the following equations:

$$\dot{Q}_{COND} = \frac{1}{2}\left[\dot{m}_{REF}(h_{REF,COND,IN} - h_{REF,COND,OUT}) + \dot{m}_W c_{P,W}(T_{W,COND,OUT} - T_{W,COND,IN})\right] \quad (1)$$

$$COP = \frac{\dot{Q}_{COND}}{\dot{W}_{COMP}} \quad (2)$$

$$\eta_{VOL} = \frac{\dot{m}_{REF}}{\rho_{REF,COMP,IN}\dot{V}_{COMP}} \quad (3)$$

$$\Delta T_{PP,EVAP} = T_{W,EVAP,OUT} - T_{REF,EVAP,IN} \quad (4)$$

$$\Delta T_{PP,COND} = T_{REF,SAT}(p_{REF,COND,IN}) - T_{W,COND,OUT} \quad (5)$$

Refprop 10.0 [16] was used to calculate all the refrigerant data and the water isobaric heat capacity.

The estimation of the uncertainty of each parameter was carried out following the procedure proposed in [17]. According to it, for the directly measured variables, the experimental uncertainty is calculated with Equation (6) considering the 900 samples recorded during each test, whereas for the calculated quantities, the uncertainty is estimated under the assumption of uncorrelated independent variables and using the combined standard uncertainty as per Equation (7). In this study, the confidence level of each parameter was 95%, resulting in a maximum uncertainty of ±137 W for the heating capacity, of ±0.1 for the COP, of ±3% for the volumetric efficiency, of ±0.1 °C for the temperatures and of ±0.15 °C for the temperature differences.

$$u_x = \pm\sqrt{u_{x,INST}^2 + (t_{95}\sigma_x)^2} \tag{6}$$

$$u_y = \pm\sqrt{\sum_{i=1}^{N}\left(\frac{\partial y}{\partial x_i}\right)^2 u_{x,i}^2} \tag{7}$$

3. Results

First, the performances at the heat pump level are discussed. As stated in Section 2.3, the parameters that are considered are the heat pump heating capacity and the COP. The condenser heat transfer rate and the COP for R1234ze(E) and R515B as a function of the temperature of water–ethylene glycol at the evaporator outlet and of the temperature of water at the condenser outlet are shown in Figures 2 and 3, respectively.

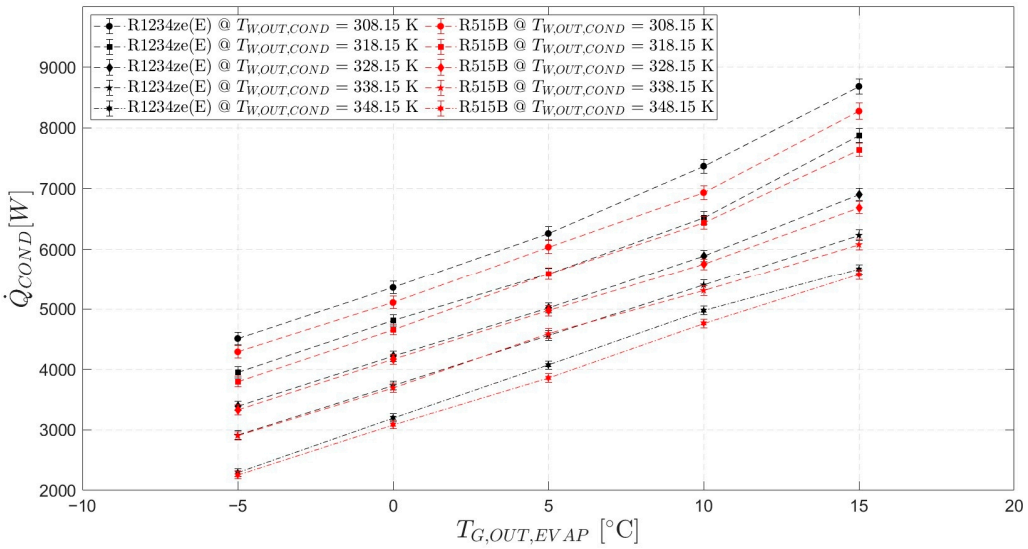

Figure 2. The condenser heat transfer rate for R1234ze(E) and R515B as a function of the temperature of water–ethylene glycol at the evaporator outlet and of the temperature of water at the condenser outlet.

The trend of these two quantities follows the well-established theoretical trend according to which both the capacity and the COP of any vapour compression system reduce with the reduction in the evaporating temperature and the increase in the condensing temperature. The former reduces when the temperature of the secondary fluid at the evaporator outlet reduces, whereas the latter increases when the temperature of the secondary fluid at the condenser outlet increases. A closer comparison between the two refrigerants reveals that the use of R515B leads to a slight reduction in both the heat pump heating capacity and the COP. Indeed, the condenser heat transfer rate of the heat pump operated with R515B is within the range of −6.81% to +2.46% with respect to that found with R1234ze(E), whereas the COP lays in the range of −2.41% to +6.29%. This may be explained considering that the measured mass flow rate of R515B is essentially equal to that of R1234ze(E), where

the differences are in the range ±1%, whereas, depending on the testing condition, the enthalpy difference across the condenser with R515B may be up to 8% lower. Consequently, the reduction in the enthalpy difference may prevail on the (possible) increase in the mass flow rate, leading to an overall lower heating capacity. On the other side, the trend about the COP may be justified considering that as shown further in the text, with R515B, the heat pump operates with lower evaporating and condensing temperatures. Since a lower evaporating temperature is detrimental for the COP but a lower condensing temperature is beneficial, the two effects tend to compensate each other, leading to a negligible variation in the COP. This is also consistent with the findings of Domanski et al. [18], according to which the COP of any vapour compression system is influenced by the critical temperature and reference isobaric specific heat of the refrigerant. For the refrigerants considered in this study, these two parameters are very similar, with a difference in critical temperature of −0.48 K and a reference isobaric heating capacity of +2.1%, respectively. Consequently, the COPs are also quite similar.

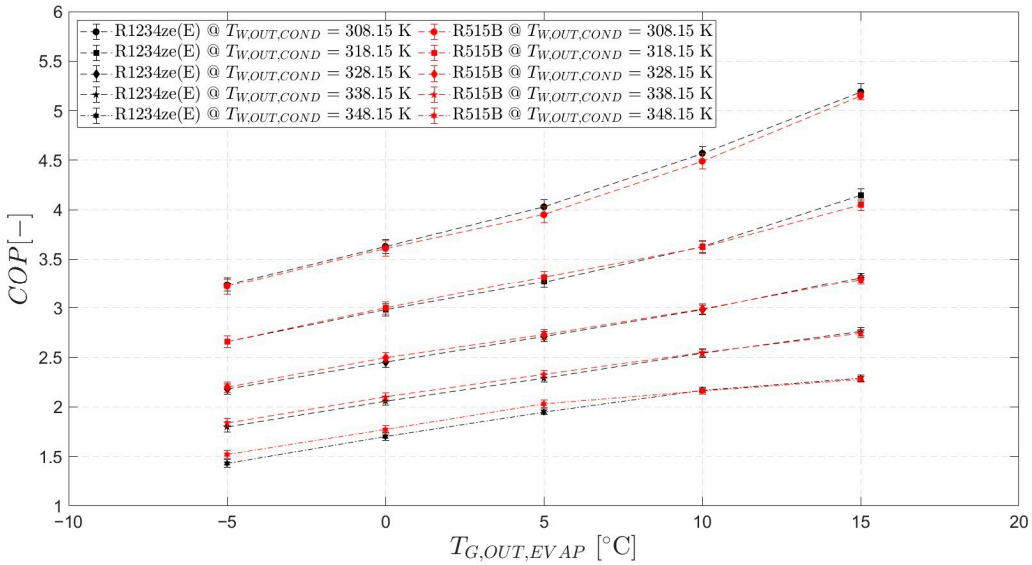

Figure 3. The COP for R1234ze(E) and R515B as a function of the temperature of water–ethylene glycol at the evaporator outlet and of the temperature of water at the condenser outlet.

Considering the component level, first, the performance of the compressor is discussed. Figure 4 shows the discharge temperature for R1234ze(E) and R515B as a function of the temperature of water–ethylene glycol at the evaporator outlet and of the temperature of water at the condenser outlet. The collected data reveal that for R515B, this parameter tends to be slightly lower than that measured with R1234ze(E), with a reduction that is in the range of −3.1 °C to −0.5 °C. This is the result of two simultaneous effects: first, as shown in Table 3, the molar mass and the reference isobaric heat capacity of R515B are slightly higher than those of R1234ze(E), which tend to reduce the temperature during the compression. Second, the pressure ratio of R515B registered during the experimental tests is slightly lower than that of R1234ze(E), which, again, tends to reduce the refrigerant temperature at the compressor discharge.

In Figure 5, the compressor volumetric efficiency as a function of the pressure ratio is reported. From the measured data, it is not possible to conclude that there is a clear difference between R1234ze(E) and R515B since the experimental results are largely overlapped, especially if the uncertainty band is considered.

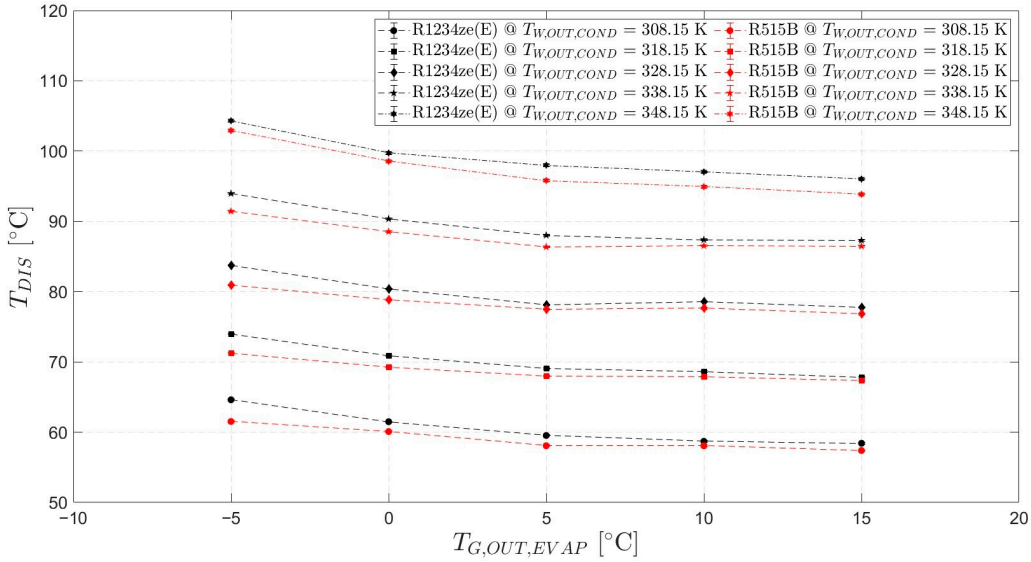

Figure 4. The refrigerant temperature at the compressor discharge for R1234ze(E) and R515B as a function of the temperature of water–ethylene glycol at the evaporator outlet and of the temperature of water at the condenser outlet.

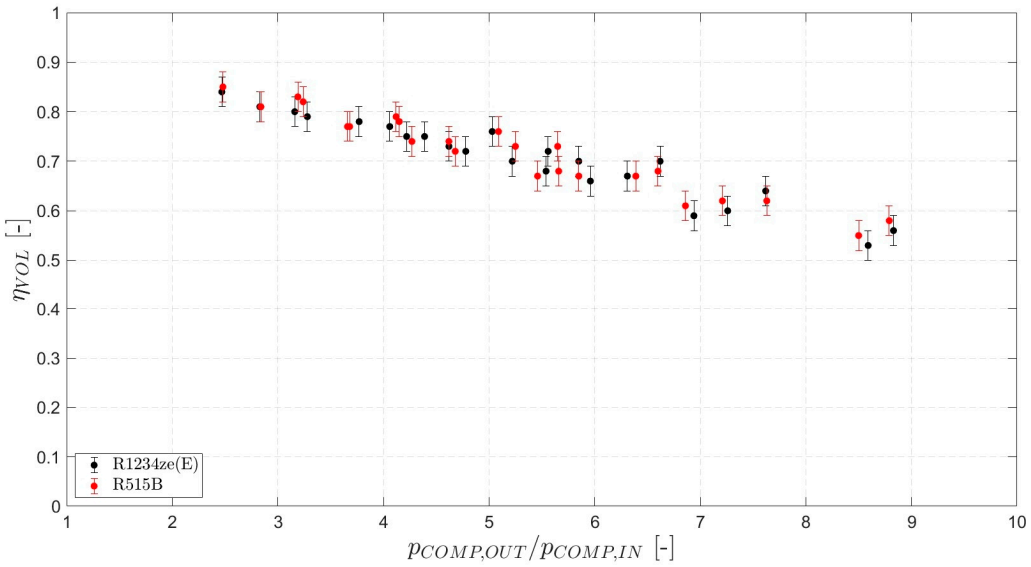

Figure 5. The compressor volumetric efficiency for R1234ze(E) and R515B as a function of the pressure ratio.

Finally, considering the two heat exchangers, the pinch points at the evaporator and at the condenser for R1234ze(E) and R515B as a function of the test number are shown in Figures 6 and 7, respectively. The collected data reveal that both the evaporating and the condensing temperatures of the heat pump working with R515B are lower than those of the heat pump working with R1234ze(E). A possible explanation of these results considers that in any heat exchanger, the pinch point is proportional to the ratio between the heat transfer rate and the overall heat transfer coefficient times the heat transfer area. The heat pump that operates with R515B transfers less heat both in the evaporator and in the condenser, as shown in Figure 2, and this is beneficial for the pinch point. However, at the same time, being a mixture, R515B exhibits an additional mass transfer resistance during phase change processes that results in a lower heat transfer coefficients, which, in turn, is detrimental for the pinch point. All-in-all, at the evaporator side, the most predominant effect is the lower overall heat transfer coefficient that leads to a higher pinch point for R515B, whereas

at the condenser side, the effect of a lower heat transfer rate prevails, resulting in lower pinch points for R515B. This is consistent with the general statement that the refrigerant heat transfer coefficient is lower during flow boiling than during flow condensation, and therefore, the mass transfer resistance has a greater impact in the former situation than in the latter.

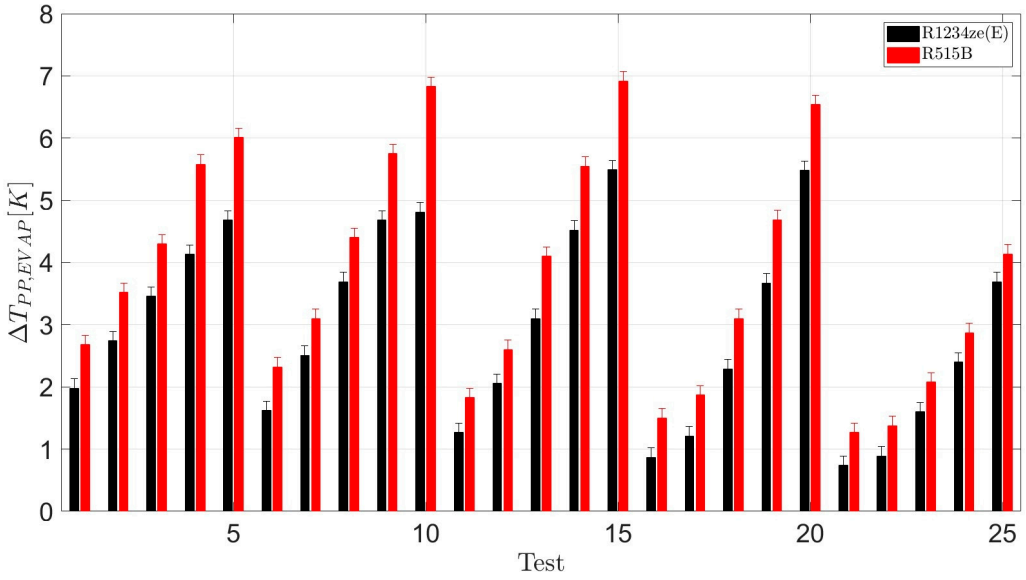

Figure 6. The pinch point at the evaporator for R1234ze(E) and R515B in the 25 experimental points.

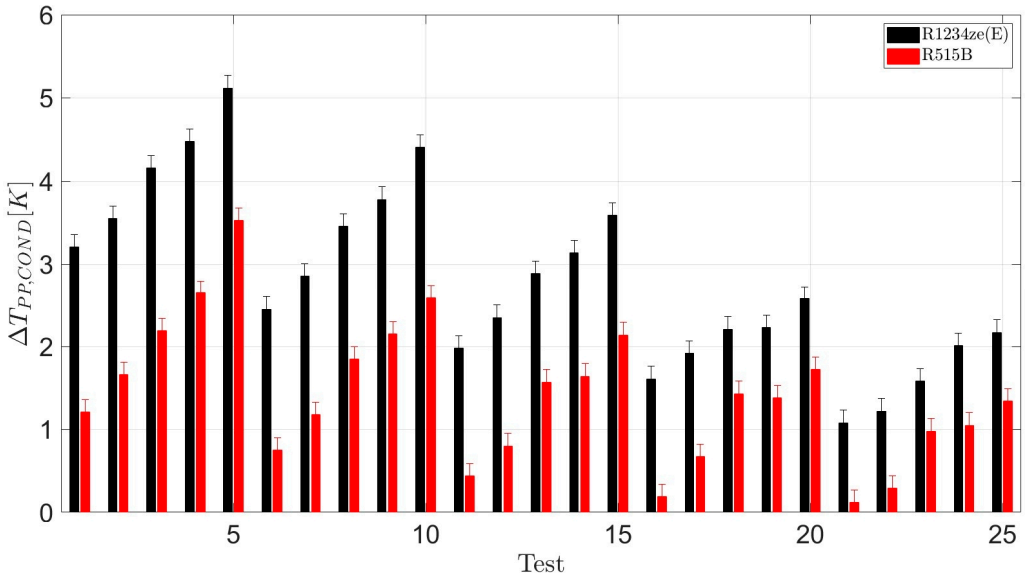

Figure 7. The pinch point at the condenser for R1234ze(E) and R515B in the 25 experimental points.

4. Conclusions

In this paper, an experimental analysis of the use of R515B in a water-to-water heat pump for drop-in application is presented. During the tests, the vapour superheating at the evaporator outlet is set to 5 K, the compressor shaft rotational frequency is fixed at 50 Hz and the temperatures of the secondary fluids at the evaporator and the condenser outlets are varied over a wide range of operating conditions. The overall performance of R515B is compared to that of R1234ze(E), the primary component of the R515B mixture.

At the system level, it is observed that using R515B results in a slight variation in heating capacity, ranging from −6.81% to +2.46%, and a variation in COP between −2.41%

and 6.29%. At the component level, from the compressor's perspective, R515B leads to slightly lower refrigerant discharge temperatures, with differences ranging from −3.09 °C to −0.49 °C, while maintaining essentially the same volumetric efficiency. Regarding the heat exchangers, R515B shows a lower pinch point in the condenser and higher pinch points in the evaporator. All-in-all, R515B seems a good alternative to R1234ze(E) at the heat pump level; an analysis at the system level (heat pump + building) is foreseen to assess the long-term performance.

Author Contributions: Conceptualisation, L.M.; methodology, L.M., A.L. and L.P.M.C.; investigation, L.M.; data curation, L.M.; writing—original draft preparation, L.M.; writing—review and editing, A.L. and L.P.M.C.; project administration, A.L. and L.P.M.C. All authors have read and agreed to the published version of the manuscript.

Funding: This study received no external funding.

Data Availability Statement: The raw data presented in this study will be made available by the authors on request.

Acknowledgments: The company Frascold S.p.A. (Rescaldina, Italy) is acknowledged for providing the compressor used in the experimental campaign. The company Nippon Gases S.r.l. (Milano, Italy) is acknowledged for providing the sample of R515B. Davide Frigerio is acknowledged for his participation in the experimental activity.

Conflicts of Interest: The authors declare no conflicts of interest.

Nomenclature

c_P	isobaric heat capacity ($J \cdot kg^{-1} \cdot K^{-1}$)
COP	Coefficient of performance (-)
h	enthalpy ($J \cdot kg^{-1}$)
$\dot{m}$	mass flow rate ($kg \cdot s^{-1}$)
$\dot{Q}$	heat transfer rate (W)
t_{95}	Student's distribution multiplier at 95% confidence level (-)
T	temperature (K)
u	uncertainty (various)
$\dot{V}_{COMP}$	compressor swept volume ($m^3 \cdot s^{-1}$)
x	directly measured quantity (various)
y	calculated quantity (various)
$\dot{W}$	power (W)
Greek symbols	
ΔT_{PP}	pinch point (K)
η_{VOL}	volumetric efficiency (-)
ρ	density ($kg \cdot m^{-3}$)
σ_x	standard deviation (various)
Subscripts	
COMP	compressor
COND	condenser
DIS	discharge of the compressor
EVAP	evaporator
IN	inlet
OUT	outlet
REF	refrigerant
SAT	saturation
W	water

References

1. European Union. Regulation (EU). No 573/2024 of the European Parliament and the council of 7 February 2024 on fluorinated greenhouse gases, amending Directive (EU) 2019/1937 and repealing Regulation (EU) No 517/2014. *Off. J. Eur. Union* **2024**, 1–67. Available online: https://eur-lex.europa.eu/eli/reg/2024/573/oj (accessed on 23 September 2024).

2. United Nations. The amendment to the Montreal Protocol agreed by the Twenty-Eighth Meeting of the Parties (Kigali, 10–15 October 2016). United Nations Climate Change, 2013. The Paris Agreement. Available online: https://unfccc.int/processand-meetings/the-paris-agreement/the-paris-agreement (accessed on 23 September 2024).
3. Ally, M.R.; Sharma, V.; Nawaz, K. Options for low-global-warming-potential and natural refrigerants part I: Constrains of the shape of the P–T and T–S saturation phase boundaries. *Int. J. Refrig.* **2019**, *106*, 144–152. [CrossRef]
4. Nawaz, K.; Ally, M.R. Options for low-global-warming-potential and natural refrigerants part 2: Performance of refrigerants and systemic irreversibilities. *Int. J. Refrig.* **2019**, *106*, 213–224. [CrossRef]
5. Calleja-Anta, D.; Nebot-Andres, L.; Cabello, R.; Sánchez, D.; Llopis, R. A3 and A2 refrigerants: Border determination and hunt for A2 low-GWP blends. *Int. J. Refrig.* **2022**, *134*, 86–94. [CrossRef]
6. Bell, I.H.; Domanski, P.A.; McLinden, M.O.; Linteris, G.T. The hunt for nonflammable refrigerant blends to replace R-134a. *Int. J. Refrig.* **2019**, *104*, 484–495. [CrossRef]
7. Mota-Babiloni, A.; Mateu-Royo, C.; Navarro-Esbrí, J.; Barragán-Cervera, Á. Experimental comparison of HFO-1234ze(E) and R-515B to replace HFC-134a in heat pump water heaters and moderately high temperature heat pumps. *App. Therm. Eng.* **2021**, *196*, 117256. [CrossRef]
8. Mateu-Royo, C.; Mota-Babiloni, A.; Navarro-Esbrí, J.; Barragán-Cervera, Á. Comparative analysis of HFO-1234ze(E) and R-515B as low GWP alternatives to HFC-134a in moderately high temperature heat pumps. *Int. J. Refrig.* **2021**, *124*, 197–206. [CrossRef]
9. Azzolin, M.; Berto, A.; Bortolin, S.; Del Col, D. Condensation heat transfer of R1234ze(E) and its A1 mixtures in small diameter channels. *Int. J. Refrig.* **2022**, *137*, 153–165. [CrossRef]
10. Diani, A.; Liu, Y.; Wen, J.; Rossetto, L. Experimental investigation on the flow condensation of R450A, R515B, and R1234ze(E) in a 7.0 mm OD micro-fin tube. *Int. J. Heat Mass Transf.* **2022**, *196*, 123260. [CrossRef]
11. Liu, Y.; Rossetto, L.; Diani, A. Flow Boiling of R450A, R515B, and R1234ze(E) Inside a 7.0 mm OD Microfin Tube: Experimental Comparison and Analysis of Boiling Mechanisms. *Appl. Sci.* **2022**, *12*, 12450. [CrossRef]
12. Colombo, L.P.M.; Frigerio, D.; Lucchini, A.; Molinaroli, L. Experimental assessment of the use of R515B as R1234ze(E) alternative in a small water-to-water heat pump. In Proceedings of the 26th International Congress of Refrigeration, Paris, France, 21–25 August 2023.
13. Janković, Z.; Sieres Atienza, J.; Martínez Súarez, J. Thermodynamic and heat transfer analyses for R1234yf and R1234ze(E) as drop-in replacements for R134a in a small power refrigerating system. *App. Therm. Eng.* **2015**, *80*, 42–54. [CrossRef]
14. Colombo, L.; Lucchini, A.; Molinaroli, L. Experimental analysis of the use of R1234yf and R1234ze(E) as drop-in alternatives of R134a in a water-to-water heat pump. *Int. J. Refrig.* **2020**, *115*, 18–27. [CrossRef]
15. Molinaroli, L.; Lucchini, A.; Colombo, L.P.M. Drop-in analysis of R450A and R513A as low-GWP alternatives to R134a in a water-to-water heat pump. *Int. J. Refrig.* **2022**, *135*, 139–147. [CrossRef]
16. Lemmon, E.W.; Bell, I.; Huber, M.L.; McLinden, M.O. NIST Standard Reference Database 23: Reference Fluid Thermodynamic and Transport Properties-REFPROP, Version 10.0, National Institute of Standards and Technology. 2018. Available online: https://www.nist.gov/srd/refprop (accessed on 18 November 2024).
17. Moffat, R. Describing the uncertainties in experimental results. *Exp. Therm. Fluid Sci.* **1988**, *1*, 3–17. [CrossRef]
18. Domanski, P.; Brown, J.; Heo, J.; Wojtusiak, J.; McLinden, M. A thermodynamic analysis of refrigerants: Performance limits of the vapor compression cycle. *Int. J. Refrig.* **2014**, *38*, 71–79. [CrossRef]